

1 **Genome-wide scans of selection highlight the impact of biotic and abiotic**
2 **constraints in natural populations of the model grass *Brachypodium distachyon*.**

3

4

5 Yann Bourgeois¹, Christoph Stritt², Jean-Claude Walser³, Sean P. Gordon⁴, John P.
6 Vogel⁴, Anne C. Roulin^{2*}

7

8

9

10 ¹ New York University Abu Dhabi, PO Box 129188, Saadiyat Island, Abu Dhabi,
11 United Arab Emirates

12 ² Institute of Plant and Microbial Biology, University of Zürich, Zollikerstrasse 107,
13 8008 Zürich, Switzerland

14 ³ Genetic Diversity Centre, ETH Zürich, Universitätstrasse 16, Zurich, Switzerland

15 ⁴DOE Joint Genome Institute, Walnut Creek, CA 94598, USA.

16

17 * Corresponding author: anne.roulin@botinst.uzh.ch

18

19 Key words: local adaptation, genome scans of selection, grasses, *Brachypodium*
20 *distachyon*, host-pathogen interaction.

21

22 **Summary**

23 Grasses are essential plants for ecosystem functioning. Thus, quantifying the selection
24 pressures that act on natural variation in grass species is essential regarding
25 biodiversity maintenance. In this study, we investigated the selection pressures that
26 act on natural populations of the grass model *Brachypodium distachyon* without prior
27 knowledge about the traits under selection. To do so, we took advantage of whole-
28 genome sequencing data produced for two natural populations of *B. distachyon* and
29 used complementary genome-wide scans of selection (GWSS) methods to detect
30 genomic regions under balancing and positive selection. We show that selection is
31 shaping genetic diversity at multiple temporal and spatial scales in this species and
32 affects different genomic regions across the two populations. Gene Ontology
33 annotation of candidate genes reveals that pathogens may constitute important factors
34 of selection in *Brachypodium distachyon*. We eventually cross-validated our results
35 with QTL data available for leaf-rust resistance in this species and demonstrated that,
36 when paired with classical trait mapping, GWSS can help pinpointing candidate genes
37 for further molecular validation. Our study revealed widespread signatures of natural
38 selection on genes involved in adaptation in *B. distachyon* and suggests that
39 pathogens may constitute an important driving force of genetic diversity and
40 evolution in this system. Thanks to a near-base perfect reference genome and the
41 large collection of freely available natural accessions collected across its natural
42 range, *B. distachyon* appears as a prime system for studies in ecology, population
43 genomics and evolutionary biology.

44

45

46 **Introduction**

47 Grasses cover more than 40% of the world land area (Gibson, 2009) and dominate a
48 wide variety of ecosystems, from tropical to temperate regions (Clayton, 1981;
49 Gibson, 2009). Grasses also play a key role in eco- and agrosystem functioning as
50 they provide habitats for many animal species (Groves, 2000) and represent the main
51 source of grain and forage (Stromberg, 2011). Increasing crop production to meet the
52 food and energy requirements of the world's growing population is however putting
53 great pressure on natural grasslands (Wallace, 1997; Helm *et al.*, 2009; Ceballos *et*
54 *al.*, 2010). Faced with constant deterioration and fragmentation due to anthropic
55 activities (Kiviniemi, 2002), these ecosystems are highly endangered (Ceballos *et al.*,
56 2010), but little is known about their evolutionary resilience. Assessing the genetic
57 basis of adaptation and quantifying the selection pressures that act on natural variation
58 in grass species is therefore crucial with respect to biodiversity maintenance and food
59 security.

60 To date, reciprocal transplant experiments have been extensively used to test the
61 effect of selection on adaptive differentiation across populations (for review see
62 Savolainen *et al.*, 2013). Based on a “home vs. foreign” effect on fitness, reciprocal
63 transplants are indeed powerful to unravel overall genotype by environment (GxE)
64 interactions and demonstrated the prevalence of local adaptation in grasses and plants
65 in general (for review see Bischoff *et al.*, 2006; Wadgyman *et al.*, 2017). However,
66 reciprocal transplant experiments use proxy such as survival, vegetative growth or
67 seed production to measure the effect of the habitat on fitness (Bischoff *et al.*, 2006).
68 Hence, they provide little information about the functional and genetic bases of
69 adaptation, unless combined with trait mapping such as quantitative trait locus (QTL)
70 analyses and genome-wide association studies (GWAS) (Latta, 2009). QTL analyses
71 and GWAS, on the other hand, are largely constrained by the effort and time
72 necessary for high-resolution mapping. In grasses, while these trait-by-trait
73 approaches have been valuable to decipher the genetic architecture of important
74 characters with regard to crop genetic improvement (Huang *et al.*, 2002; Barbieri *et*
75 *al.*, 2012; Morris *et al.*, 2013; Slavov *et al.*, 2014), they remain of limited value to
76 grasp the overall selective forces that act on natural populations.

77 An efficient alternative to provide insights about evolutionary forces in natural
78 populations consists in identifying genes under various types of selection at a whole

79 genome scale, then describing their function and the type of selection acting on them
80 (Mitchell-olds *et al.*, 2007). For instance, new mutations that are beneficial in some
81 populations will be positively selected and are more likely to quickly increase in
82 frequency. Such so-called selective sweeps tend to reduce genetic diversity, increase
83 differentiation among populations, and lead to extended haplotypes in the vicinity of
84 the locus under selection due to genetic hitchhiking (Nielsen, 2005; Hermisson,
85 2009). Various genome-wide selection scans (GWSS) methods have been developed
86 to detect such footprints of positive selection in genomes while taking into account
87 demographic history (Tang *et al.*, 2007; Gautier *et al.*, 2012; Stamatakis *et al.*, 2013;
88 Messer, 2015), and thanks to the remarkable progress of sequencing technologies,
89 GWSS are now emerging as complementary approaches to classical trait mapping.

90 While local adaptation is commonly associated to positive selection on new
91 advantageous polymorphisms, recent studies have demonstrated that balancing
92 selection is also playing an important role in this evolutionary process (Mitchell-Olds
93 *et al.*, 2007; Rasmussen *et al.*, 2014; Wu *et al.*, 2017). The term balancing selection is
94 an “umbrella” concept (Fijarczyk & Babik, 2015) which describes the maintenance of
95 genetic diversity over longer periods of time through adaptation to spatial
96 heterogeneity, heterozygote advantage and negative frequency-dependent selection
97 (Mitchell-Olds *et al.*, 2007; Rasmussen *et al.*, 2014). Leading to the recycling of
98 polymorphisms and to selection on standing variation (Richman, 2000; Turchin *et al.*,
99 2012), this process is more difficult to detect than positive selection (Fijarczyk &
100 Babik, 2015) since older alleles had more time to recombine and may lead to narrow
101 signatures around selected sites. As a consequence, the effect of balancing selection is
102 still largely overlooked in genome scans, which remain strongly biased towards the
103 detection of recent positive selection (Hassl & Payseur, 2016).

104 In this study, we capitalize on the near base-perfect quality of the reference genome of
105 the Mediterranean grass *Brachypodium distachyon* (<https://phytozome.jgi.doe.gov>) to
106 investigate how both positive and balancing selection are shaping diversity in this
107 species. In the last decade, *B. distachyon* has been developed as a powerful model for
108 research on temperate grass species as it is closely related to major crop cereals and to
109 some of the grasses used for biofuel production (The international brachypodium
110 Consortium, 2010). Entirely sequenced, its small diploid genome (272Mb) is fully
111 assembled into five chromosomes and has been exhaustively annotated (The

112 international brachypodium Consortium, 2010). In addition, *B. distachyon* is broadly
113 distributed around the Mediterranean rime (Dell'Acqua *et al.*, 2014; Gordon *et al.*,
114 2014; Tyler *et al.*, 2016), providing access to natural populations from contrasting
115 habitats for which a large collection has been collected. It constitutes therefore a
116 unique and prime system to investigate the genetic basis of local adaptation in natural
117 grass populations, opening the way to further fundamental and applied research.

118 Here, we took advantage of whole-genome sequencing data produced for 44
119 *B. distachyon* natural accessions originating mainly from Spain and Turkey (Gordon
120 *et al.*, 2017). We identified over 6 million SNPs and used four complementary GWSS
121 methods to detect genomic regions under different regimes of selection (Figure 1).
122 Namely, we asked i) at what time and geographical scale is selection acting in
123 *B. distachyon* populations? ii) what are the selective constrains that shape diversity
124 and adaptation in these populations? iii) whether positive selection is acting on the
125 same genomic regions in the two populations or, on the opposite, on distinct loci?

126

127

128 **Results**

129 *Population structure*

130 In this study, we used whole-genome sequencing data (paired-end; Illumina
131 technology) with a 86-fold median coverage of 44 *B. distachyon* accessions
132 originating from Turkey, Iraq, Spain and France (Figure 2A, Table S1, (Gordon *et al.*,
133 2017). After filtering, we identified 6,204,029 SNPs. An ADMIXTURE analysis,
134 where K=2 was identified as the best model, highlighted two distinct genetic clusters,
135 an eastern and a western one, with extremely little admixture between the two (Figure
136 2B). For the rest of the study, accessions from Turkey and Iraq will be referred to as
137 the eastern population while accessions from Spain and France will be referred to as
138 the western population. The western population showed a lower level of nucleotide
139 diversity (Wilcoxon test; P-value < 2.2e-16, Figure 2C) and haplotype diversity (P-
140 value < 2.2e-16, data not shown) than the eastern one. Excluding the reference
141 accession Bd21, which has been artificially inbred before sequencing, the average
142 level of heterozygosity in these accession is of 8% and ranges from 4 to 17.4% (Table
143 S1).

144 *Functional clustering of the genome of B. distachyon*

145 GWSS outputs provide information about the likelihood for a given locus to be under
146 selection. A classical approach applied to analyze the results of GWSS consists in
147 selecting genomic regions containing top 1% outliers for signals of selection and then
148 assessing whether some biological functions or processes are significantly over-
149 represented in the gene sets under selection through a Gene Ontology (GO)
150 annotation (Kelley *et al.*, 2006; Hancock *et al.*, 2011; Nelson *et al.*, 2017). While
151 recombination rate is relatively high in *B. distachyon* (Huo *et al.*, 2011), signals of
152 selection around focal loci may decrease slowly due to locally stronger linkage
153 disequilibrium and subsequent genetic hitchhiking. 1% outlier regions may thus
154 contain several adjacent genes. Because genes having the same function or being
155 involved in the same biological process tend to be physically clustered (Hammond-
156 kosack & Jones, 1996; Michelmore & Meyers, 1998; Takos *et al.*, 2011; Nutzmann &
157 Osbourn, 2014; Singh *et al.*, 2015), we anticipated that this non-random organization
158 of genomes could lead to an over-representation of some biological pathways or
159 functions in small genomic regions and to an artificial enrichment for some GO terms
160 in GWSS 1% outlier regions (Pavlidis *et al.*, 2012).

161 To assess whether the genome of *B. distachyon* harbors such functional clusters of
162 genes, we first performed a GO annotation for the 32,712 genes annotated in the
163 reference genome. We then controlled for potential gene clustering by following the
164 procedure described in (Al-Shahrour *et al.*, 2010). Briefly, we split the genome into
165 overlapping windows of 50 consecutive genes and performed enrichment analyses on
166 each window. We identified 272 windows significantly enriched for at least one
167 biological process (Table S2). Several windows were enriched for processes that may
168 be associated to adaptation to local environmental conditions such response to stress
169 and defense response (Table S2). This prompted us to narrow down top 1% outlier
170 regions by keeping only the genes located at and in the immediate vicinity (-10% of
171 the peak value) of each of the peaks of selection. With the exception of the
172 coalescence analysis, which is a window-based approach (see methods), all analyses
173 subsequent to GWSS reported in the following sections were performed on these
174 filtered outputs.

175
176

177 *Genes under balancing selection due to environmental heterogeneity*

178 Variation in abiotic conditions can drive local adaptation at a fine-grained spatial
179 scale and lead to correlations between genotypes and environment. We first used an
180 environmental association analysis approach to detect loci that may have been
181 repeatedly selected by convergent climatic conditions across the two populations. If
182 alleles at these loci have been recycled in front of environmental conditions common
183 to Spain and Turkey, they should display a detectable signal of association at the scale
184 encompassed by our study. Note that geographically varying selection is sometimes
185 considered as being distinct from balancing selection. While it can also be referred to
186 as local adaptation in the literature (Mitchell-olds *et al.*, 2007), we kept it here under
187 the term of balancing selection.

188 To detect such loci and to highlight alleles shared between the two populations, we
189 selected seven bioclimatic variables showing variation within both the eastern and
190 western populations but little variation between them (Figure 2D). As all these
191 variables were either associated to temperature or to precipitation and are likely to be
192 correlated, we summarized them with a PCA. The first axis of the PCA explained
193 62.6% of the variance but did not discriminate populations (Figure 2D) and was used
194 to perform an environmental association analysis with all the SNPs identified across
195 the 44 accessions. We identified 26 genomic regions associated with the first PCA
196 axis. These regions harbored 71 genes (Figure 3A). No significant enrichment for any
197 specific biological process was observed (Table 1).

198

199 *Genes harboring extremely long coalescence time*

200 Balancing selection can be detected with coalescence approaches, as ancient alleles
201 are associated with older coalescence times (Charlesworth, 2006). To detect
202 additional candidate regions for balancing selection in *B. distachyon*, we used the
203 software ARGWeaver (Rasmussen *et al.*, 2014). Briefly, ARGWeaver models the
204 coalescent process along chromosomes and across non-recombining blocks of
205 sequences to address their evolutionary history. It allows recovering several statistics
206 that describe local genealogies and recombination, such as times since the most recent
207 common ancestor (TMRCA), which should be increased near ancient alleles such as
208 those under ancient balancing selection. By doing so, we identified 72 regions
209 harboring 115 genes under what will be referred to as long-term balancing selection in

210 the following. We observed a significant enrichment for genes involved in
211 phosphorylation (Table 1).

212

213 *Genes under disruptive selection between western and eastern populations*

214 As new mutations providing a selective advantage rise in frequency through positive
215 selection, neutral mutations that are physically close tend to remain strongly linked to
216 them. Recent positive selection should therefore lead to a signature of long haplotypes
217 near selected mutations. We used the Rsb test (Tang *et al.*, 2007) to detect such
218 signatures of recently or almost completed selective sweeps. This test detects
219 haplotypes that are positively selected in one population by estimating the length of
220 haplotypes around each allele at a core SNP, then comparing these lengths between
221 populations. In contrast to the two approaches presented above, the Rsb test should
222 detect regions that are genetically differentiated across the two populations (Figure 1).
223 We identified 312 regions harboring 824 genes and 319 regions harboring 1212 genes
224 in the eastern and western populations respectively (Figure 3A). The selected regions
225 contained more genes in the western than in the eastern population (Wilcoxon test, P-
226 value=0.001; Figure 3B). We observed a significant enrichment in genes involved in
227 response to stress, particularly for defense response and response to oxidative stress in
228 the eastern population (Table 1, Table S3). The gene set associated to the process of
229 defense response contained well-known types of resistance genes (R-genes), i.e genes
230 with NBS-LRR domains (Table S3). Eventually, we observed a significant
231 enrichment for genes involved in nitrogen transport in the western population (Table
232 1, Table S3).

233

234 *Genes under ongoing selection within population*

235 In the case of an ongoing and partial selective sweep (Figure 1), not all individuals
236 within the population will display haplotype extension in the region under selection,
237 which can lead to more subtle patterns that are not detected by Rsb test. We used the
238 program H-scan to detect such incomplete patterns and genes under ongoing positive
239 selection. We identified 142 regions harboring 487 genes and 79 regions harboring
240 463 genes in the eastern and western population respectively (Figure 3A). The gene
241 set under selection in the eastern population was significantly enriched for genes
242 involved in stress response, including the processes of defense response and response

243 to cadmium ion (Table 1). The gene set associated to the process of defense response
244 also contained many R-genes (Table S3). The gene set under selection in the western
245 population showed a significant enrichment for genes involved in pyruvate metabolic
246 process (Table 1, Table S3). As in the previous Rsb analysis, the selected windows
247 contained more genes in the western than in the eastern population (Wilcoxon test, P-
248 value=0.003; Figure 3B).

249

250 *GWSS outliers display allele frequency spectra and coalescence patterns consistent*
251 *with expectations*

252 To test whether candidate regions displayed an allele frequency spectrum consistent
253 with the type of selection they were supposed to detect, we computed different
254 statistics and compared candidate regions to the rest of the genome. We first
255 computed Tajima's D (Tajima, 1989), which is a measure of genetic diversity
256 influenced by both selection and demographic variation. Positive values are
257 associated with balancing selection and bottlenecks, while negative values suggest
258 recent expansion or positive/purifying selection. We then computed nucleotide
259 diversity, genome-wide relative (F_{ST}) and absolute (d_{XY}) measures of population
260 differentiation (Cruickshank & Hahn, 2014). Note that d_{XY} can be interpreted as F_{ST} ,
261 but is correlated to the time to coalescence of alleles from all populations, making it
262 independent of diversity within populations. In addition to TMRCA values, we finally
263 extracted relative TMRCA halftime (RTH) values from the output of ARGWeaver.
264 RHT captures coalescence events are skewed toward the recent past but is
265 independent of the overall coalescence rate (Rasmussen *et al.*, 2014). Assuming
266 similar selection strength acting on Rsb and H-scan outliers, RTH is thus expected to
267 be smaller in regions under ongoing positive selection (H-scan) than in regions under
268 disruptive selection where one allele already reached near-fixation in one of the two
269 populations (Rsb).

270 Regions associated with bioclimatic variables or under long-term balancing selection
271 displayed significantly higher Tajima's D than the genomic background (Wilcoxon
272 test, all P-values < $1.0 \cdot 10^{-10}$, Figure 3C) except for associated loci in Spain for which
273 Tajima's D values were only marginally higher than in the rest of the genome (P-
274 value=0.055). These regions also display a significantly higher level of nucleotide
275 diversity within regional groups (P-values < $1.0 \cdot 10^{-10}$) than the rest of the genome.

276 Coalescence times (TMRCA) within regional groups were higher for windows
277 covering loci associated to environmental variables than for genomic background (P-
278 values= 1.10^{-14} and 0.02 for eastern and western populations respectively). As
279 expected, regions under long-term balancing selection also displayed higher
280 TMRCA as they were specifically selected as belonging to the top 1% outlier for this
281 statistic. Tajima's D, nucleotide diversity and TMRCA statistics are thus consistent
282 with our expectations and confirmed that both the environmental association and
283 coalescence analyses detected older polymorphisms shared across the two
284 populations.

285 On the other hand, regions identified with the H-scan and Rsb approaches harbored
286 negative and significantly lower Tajima's D than the rest of the genome, which is
287 consistent under positive selection (all P-values $< 1.10^{-5}$, Figure 3C). Outlier windows
288 for Rsb also displayed higher relative (F_{ST} , P-values $< 2.2.10^{-16}$) and absolute levels of
289 differentiation (d_{XY} ; P-values $< 2.2.10^{-16}$) than the rest of the genome. These latter
290 patterns are coherent with the high frequencies of divergent haplotypes between the
291 western and eastern population for Rsb outliers, resulting in an increased
292 differentiation between them (Figure 1). H-scan and Rsb outliers also displayed a
293 lower RTH compared to genomic background (all P-values $< 2.2.10^{-16}$ except for
294 Turkish Rsb outliers for which P-value = 0.002), which is also consistent with
295 selective sweeps where selection skews coalescence times towards the recent past for
296 most (but not necessarily all) lineages (Rasmussen *et al.*, 2014). Eventually, H-scan
297 outliers displayed lower RTH than Rsb outliers (all P-values $< 2.2.10^{-16}$), which
298 confirms that this test tended to detect more recent sweeps than the Rsb.

299

300 *Overlap between outputs from the four different approaches*

301 As expected given the specificity of each test, we found little overlap between the
302 outputs of the four different tests (Figure 3A). Out of a total of 1,262 and 1,617 genes
303 under positive selection, only 49 and 58 genes were common to the H-scan and Rsb
304 approaches in the eastern and the western population respectively. Similarly, little
305 overlap (10 genes in total) was observed between the environmental association
306 analysis and the Rsb or H-scan tests (Figure 3A). No overlap was observed between
307 the gene sets detected to be under selection with the coalescence approach and with
308 any the three other tests.

309 *Genomic regions affected by positive selection*

310 We also tested whether distinct loci/genomic regions were affected by recent positive
311 selection (Rsb and H-scan outliers combined) in the two populations using linear
312 models. We found no association between the density of genes under selection in the
313 eastern and western populations on chromosomes 2 and 3 (p-value = 0.4 and 0.3
314 respectively), which indicates that, as observed on Figure 3D, distinct regions are
315 affected by positive selection on these two chromosomes. We found a significant
316 association between these variables on chromosomes 1, 4 and 5 (p-value = 0.004,
317 1.07e-11 and 0.02 respectively). In these latter cases, however, R^2 were small (7.366e-
318 05, 0.0004 and 4.42e-05) suggesting that many regions affected by selection remain
319 specific to each population on these chromosomes as well, as depicted on Figure 3D.

320

321 *Identification of candidate genes in known QTL regions*

322 Combining association mapping and analyses of selection constitutes a powerful
323 approach to identify candidate genes and to address their selective regime. We
324 identified many candidate regions harboring resistance genes. As a proof of concept,
325 we aimed at assessing whether regions identified as resistance loci against known
326 pathogens were also highlighted in our scans of selection. In *B. distachyon*, the
327 genetic basis of resistance to the rust fungus *Puccinia brachypodii* has been
328 deciphered through a QTL mapping (Barbieri *et al.*, 2012) which showed that leaf-
329 rust resistance is controlled by three main QTL located on chromosome 2 (from
330 nucleotide 37,949,269 to 40,903,216), 3 (from nucleotide 13,943,000 to 14,512,222)
331 and 4 (from nucleotide 9,649,152 to 10,679,750). For the rest of the study, these
332 regions will be referred to as QTL_{rust-2}, QTL_{rust-3} and QTL_{rust-4}.

333 We screened these three regions for evidence of selection and found strong Rsb
334 signals in QTL_{rust-3} and QTL_{rust-4} (Figure 4A). These regions were not detected as
335 outliers with any other test but belonged to the top 0.05% p-values of Rsb outliers.
336 The Rsb signal in QTL_{rust-3} reaches its highest point in a serine/threonine phosphatase
337 (Bradi3g16320: 14,486,831- 14,488,838; Figure 4A, left panel) and 60 kb upstream
338 the QTL peak identified in this region (Barbieri *et al.*, 2012). The two adjacent Rsb
339 signals in QTL_{rust-4} reach their highest point into two NBS-LRR resistance genes
340 (Bradi4g10153: 9,807,879-9,812,927; and Bradi4g10171: 9,828,236-9,835,003;
341 Figure 3A, right panel). These two genes are respectively located 6 kb and 22 kb

342 upstream the QTL peak. We observed extended haplotypes in the eastern population
343 in both QTL_{rust-3} and QTL_{rust-4} (Figure 4B). Congruent with the signal detected by the
344 Rsb test, the large majority of the eastern accessions displayed the extended haplotype
345 in these regions, indicating a nearly completed selective sweep, especially in QTL_{rust-4}
346 (Figure 4B).

347 QTL_{rust-4} showed a striking enrichment for genes involved in defense response
348 (displayed by grey boxes in Figure 4A, P-value = 8E-09) and in immune signaling
349 process such as phosphorylation (P-value = 5.6E-06). Among 113 genes covered by
350 QTL_{rust-4}, 40 correspond either to a gene with a NBS-LRR, a receptor-like protein
351 kinase (RLK) or a F-box domains, three types of genes that can confer resistance in
352 plants. The presence of such a large gene clusters, as found in other regions of the
353 genome (Table S2), further demonstrates the importance of narrowing down regions
354 under selection to top outlier genes for unbiased GO annotation.

355

356

357 **Discussion**

358 Assessing the time and spatial scales at which selection acts is a key to understand
359 how genetic diversity is maintained or lost through adaptation (Stinchcombe &
360 Hoekstra, 2008; Fuller *et al.*, 2015). In plants, and especially in grasses, this question
361 has been largely restricted to crops, which biases our understanding of evolutionary
362 processes that have shaped genomes in their natural ancestors and extant relatives. In
363 this study, we investigate the selective forces influencing adaptation in two
364 populations consisting of 44 natural accessions of the wild Mediterranean grass
365 *B. distachyon*. We found that ancient balancing and recent positive selection left
366 distinct signatures on specific gene categories, and that positive selection affects
367 distinct loci across the two populations. Importantly, our results support a role for
368 pathogens in driving population differentiation and confirm that GWSS constitute
369 effective approaches to pinpoint candidate genes as a complement to classical trait
370 mapping.

371

372 *Time- and space-varying selection is shaping diversity in B. distachyon*

373 The ending of the last glaciation period 10,000 years ago led to drastic and recent
374 changes of plant communities in Eurasia (Svenning *et al.*, 2008; Binney *et al.*, 2017).

375 At that time, climate warmed and species distribution expanded over Europe (Hewitt,
376 1999). Pollen-based studies show that vegetation expansion was fast, reaching up to
377 2km per year for some species (Hewitt, 1999). To our knowledge, no fossil pollen
378 records are available for *B. distachyon*, which prevents reconstructing the
379 geographical distribution of this species before and during the last ice age. Yet, a
380 previous study showed that the two populations analyzed here experienced a severe
381 population size reduction during the last glaciation followed by a rapid expansion
382 within the last 10,000 years (Stritt *et al.*, in press). Even though unraveling the history
383 of populations in southern peninsulas is more complex than in northern regions
384 (Hewitt, 2000; Feliner, 2011), these results are congruent with the recent global
385 postglacial recolonization of Europe by plants (Hewitt, 1999; Svenning *et al.*, 2008;
386 Binney *et al.*, 2017) and imply that *B. distachyon* populations had to adapt to newly
387 colonized habitats in the recent past.

388 Balancing selection associated to spatial heterogeneity (Richman, 2000;
389 Charlesworth, 2006; Fijarczyk & Babik, 2015; Wu *et al.* 2017) may have maintained
390 ancestral polymorphisms over long periods of time in natural populations of
391 *B. distachyon*. Our environmental association analysis indeed shows that loci
392 associated to bioclimatic variables display higher diversity, older alleles and more
393 shared variation between regional groups when compared to genomic background.
394 We exclusively focused the analysis on bioclimatic variables that displayed variation
395 across localities and not between (Figure 2D). This approach, together with our
396 relatively small sample size, could explain why this analysis highlighted fewer genes
397 than the other methods used in the rest of the study. Our observations nonetheless
398 suggest that adaptation to climate after recolonization does not necessarily involve *de*
399 *novo* mutations, even after strong bottlenecks. As a further support of balancing
400 selection, we identified an even older set of shared polymorphisms with a coalescence
401 approach. The environmental heterogeneity encountered by *B. distachyon* populations
402 (Lopez-Alvarez *et al.*, 2015) thus seems to have provided selective pressure strong
403 enough to maintain polymorphisms over long periods of time within each population.
404 This result is congruent with a previous analysis of natural populations of
405 *B. distachyon* originating exclusively from Turkey (Dell'Acqua *et al.*, 2014) which
406 showed, at a smaller geographical scale than the one investigated here, that
407 populations are adapted to local habitats (Dell'Acqua *et al.*, 2014).

408 On the other hand, we also found evidence for positive selection acting on younger
409 polymorphisms with both the Rsb and H-scan tests. These tests also revealed that
410 positive selection is targeting different loci in the two populations. Interestingly, these
411 loci appear to be non-randomly distributed along chromosomes (Figure 3D). As
412 recombination rate is relatively high in *B. distachyon* (Huo *et al.*, 2011), we do not
413 believe that this pattern is due to extended linkage disequilibrium and the subsequent
414 process of linked selection along such large genomic regions (Cutter & Payseur,
415 2013; Slotte, 2014). Rather, the peaks of selection we identified were narrow and
416 allowed to pinpoint genes (Figure 4), indicating that while *B. distachyon* is primarily
417 inbreeding, outcrossing events must be frequent enough to limit extended linkage
418 disequilibrium. This is also congruent with the higher level of heterozygosity we
419 observed here in *B. distachyon* compared to other selfing plants such as *A. thaliana*
420 (Platt *et al.*, 2010). Whether these regions form islands of divergence and result from
421 a complex interaction between recombination rate variation, gene flow and selection
422 (Renaut *et al.*, 2013; Samuk *et al.*, 2017) remains to be investigated. As we obtained
423 enrichments for different GO terms in the eastern and western populations, our study
424 nonetheless shows that contrasting abiotic and biotic factors are shaping population
425 diversity at different regions of the genome of *B. distachyon* through positive
426 selection.

427 *B. distachyon* occurs exclusively in Mediterranean habitats which may appear at a
428 first glance to be homogeneous and unlikely to promote local adaptation. Our results
429 defeat this prediction and revealed that natural selection affected different genes and
430 genomic regions across populations. Even though we identified more genes under
431 positive than under balancing selection, it would be daring to conclude that the former
432 selection regime, less challenging to detect (Delph & Kelly, 2014), is a predominant
433 process shaping diversity in this species. Rather, we believe that we provide here
434 genomic evidence that large-scale balancing selection also leads to the adaptation of
435 *B. distachyon* populations to local environmental conditions.

436

437 *Pathogens as a potential driving force of population evolution*

438 Host-pathogen interactions lead to a strong coevolutionary dynamics and are
439 considered as a major factor shaping diversity (Karasov *et al.*; Fumagalli *et al.*, 2011;
440 Krattinger & Keller, 2016a). Two main types of interaction have been proposed.

441 Under an arms race model, repeated innovation from both sides results in repeated
442 fixation of advantageous alleles (Brown & Tellier, 2011). This interaction can
443 therefore lead to positive selection that can be detected by tests focusing on extended
444 haplotypes. The other type of interaction is often referred to as Red Queen dynamics
445 or trench warfare, where alleles involved in the interaction are recycled by negative-
446 frequency dependence and can therefore subsist for long periods of time in
447 populations through balancing selection (Brown & Tellier, 2011).

448 Plant immune system machinery is complex. On one hand, it is composed of two tiers
449 of extracellular and intracellular receptors (Krattinger & Keller, 2016a,b) that
450 efficiently detect the presence of pathogens and constitute a first level of defense (for
451 review Greeff *et al.*, 2012; Couto & Zipfel, 2016; Eckardt, 2017). Further
452 mechanisms, such as oxidative bursts which are produced at an early stage in case of
453 pathogen invasion, can act as additional levels of defense and prevent pathogen
454 proliferation (Wojtaszek, 1997; Torres *et al.*, 2006; Fones & Preston, 2011; Sewelam
455 *et al.*, 2016). In this study, we found a significant enrichment of signals of selection at
456 genes involved in these two levels of defense in the eastern population. More
457 specifically, we found many of well-characterized R-genes, i.e. genes displaying
458 NBS-LRR domains (Mchale *et al.*, 2006; Jacob *et al.*, 2013; Liu *et al.*, 2014; Couto &
459 Zipfel, 2016; Eckardt, 2017; Ooijen *et al.*, 2017), and genes involved into oxidative
460 stress response to be under ongoing and/or disruptive selection in the eastern
461 population (Table 1). On the other hand, we also found additional R-genes and genes
462 involved in phosphorylation, a process especially important for immune signaling
463 response in plants (for review Park *et al.*, 2012), to be under balancing selection. Our
464 results are thus consistent with the two classical models of host-pathogens
465 coevolution (Mondragón-palomino *et al.*, 2002; Mchale *et al.*, 2006; Gos *et al.*, 2012;
466 Mace *et al.*, 2014; Zhong *et al.*, 2015; Wu *et al.*, 2017). Overall, and as shown in
467 other organisms (Karasov *et al.* 2014; Fumagalli *et al.*, 2011; Krattinger & Keller,
468 2016a,b; Bourgeois *et al.*, 2017), our genome-wide approach suggests that pathogens
469 may constitute an important driving force of population and genome evolution in
470 *B. distachyon*.

471 Surprisingly, the significant enrichments for resistance genes in the Rsb and H-scan
472 outlier gene sets were only observed in the eastern population. The geographical
473 origin of the populations could play a role in this pattern. The Middle East is indeed

474 the center of origin of many grasses, including *B. distachyon*, and of their associated
475 pathogens (Wyand & Brown, 2003; Stukenbrock *et al.*, 2005; Opanowicz *et al.*, 2008;
476 Hovmøller *et al.*, 2011). Many studies found that both resistance genes in plants and
477 effector genes in pathogens can be organized in clusters evolving through an arm race
478 resulting in a gene birth-and-death process (Michelmore & Meyers, 1998; Dong *et al.*,
479 2015; Singh *et al.*, 2015). Because centers of origin are usually associated to higher
480 diversity, it is therefore possible that a higher level of pathogen diversity drove
481 selection at a larger number of resistance genes in the eastern population.

482 We can, however, not rule out technical biases inherent to the sampling design and to
483 the history of the studied populations. The western population indeed experienced a
484 stronger bottleneck than the eastern one (Stritt *et al.*, in press), which, together with
485 the smaller geographical area sampled, may be responsible for the reduced nucleotide
486 and haplotype diversity we observed in this population. In addition, the bottleneck
487 may have led to longer haplotypes in the western population, which could explain
488 why windows under positive selection were on average larger and contained more
489 genes in this population than in the eastern one. Discriminating the effect of selection
490 from the one of demography remains difficult in such bottlenecked populations (Long
491 *et al.*, 2013). As a consequence, confounding effects may have resulted in the
492 detection of more false positives and blurred the GO annotation in the western
493 population. As we applied stringent filtering criteria and used approaches which are
494 expected to be robust to demographic history (Tang *et al.*, 2007), we nonetheless
495 believe that we provide the community with a reliable set of candidate loci, even for
496 the western population. It is worth noting that, despite no significant enrichment for
497 defense response, footprints of positive selection at R-genes were also found in the
498 western population. This indicates that while milder, pathogens may constitute a
499 selection pressure in this population as well.

500

501 *GWSS as complementary approach to QTL and GWAS*

502 Disentangling the mechanisms that promote or prevent adaptation requires more
503 integrated studies, using both experimentations in controlled conditions and methods
504 to characterize genetic diversity in natural populations (Feder & Mitchell-olds, 2003;
505 Stinchcombe & Hoekstra, 2008; Flood & Hancock, 2017). Several studies used
506 GWSS to validate genes functionally characterized or previously identified through

507 GWAS and to propose stronger hypotheses on the mode of selection operating on
508 traits relevant for adaptation (Roulin *et al.* 2016; Tang *et al.*, 2007; Fumagalli *et al.*,
509 2011; Bourgeois *et al.* 2017). Following this idea, we inspected three QTL regions
510 responsible for the resistance of *B. distachyon* to the leaf-rust fungus *Puccinia*
511 *brachypodii*, a natural pathogen of *B. distachyon* expected to exert strong selection on
512 natural accessions.

513 For two of these QTL regions, we found strong Rsb outliers and reduced haplotype
514 diversity in the eastern cluster in the vicinity of the QTL peaks, but no sign of
515 balancing selection. These results strongly indicate that large-scale positive selection
516 is shaping rust resistance in *B. distachyon* natural populations, as suggested in other
517 species (Dodds & Thrall, 2009; Chavan *et al.*, 2015). Interestingly, the QTL region
518 identified on chromosome 3 displays a strong signal of selection in a serine/threonine
519 phosphatase, a class of genes known for their role in defense response and stress
520 signaling (País *et al.*, 2009; Durian *et al.*, 2016). The region identified on
521 chromosome 4 is more complex and consists of a cluster of resistance and stress
522 signaling genes. Nevertheless, and while other genes display evidence of positive
523 selection, a strong peak of selection co-localizes with the peak of the QTL and points
524 at two R-genes. Such genes have been shown to confer resistance to rust in other
525 species (Bettgenhaeuser *et al.*, 2014) and constitute prime candidates for further
526 functional characterization.

527 *B. distachyon* is closely related to major crop cereals as well as to grass species used
528 for biofuel production. Translating research from *B. distachyon* to plants of
529 agronomical and economical interest will require a deeper understanding of the
530 genetic architecture of traits involved in the response to environmental stresses. The
531 molecular basis of tolerance to various abiotic stresses such as drought, salt and cold
532 has been investigated in this species (Luo *et al.*, 2011; Manzaneda, 2013; Carmo &
533 Charron, 2014; Gordon *et al.*, 2014; Marais & Juenger, 2015; Sun *et al.*, 2015; Mur &
534 Bosch, 2016). Here, we also highlighted cadmium pollution as a potential factor of
535 selection in the eastern population. As pollution with heavy metals including
536 cadmium has been reported in Turkey in regions where accessions were collected for
537 this study (Bakirdere & Yaman, 2008; Mor & Ceylan, 2017), our results suggest that
538 *B. distachyon* could be used to investigate the tolerance to this stress. As genetic
539 transformation is highly efficient in this species relative to other grasses, we anticipate

540 that combining classical trait mapping analyses with GWSS will assist allele mining
541 for additional eco-responsive traits.

542

543 *Conclusion*

544 Our results revealed widespread signatures of natural selection at genes involved in
545 adaptation in *B. distachyon*. We also found that pathogens may constitute an
546 important driving force of genetic diversity and evolution in this system. While we
547 limited our analysis to classical point mutations, recent studies showed that copy
548 number variants (CNVs) and transposable element polymorphisms are abundant
549 across *B. distachyon* populations (Gordon *et al.*, 2017; Stritt *et al.*, in press). Hence,
550 the important genomic resources currently developed in this species open new
551 avenues of research to further investigate the role of structural variation in natural
552 population evolution and adaptation. To date, *B. distachyon* remains a classical model
553 for research on grass genomics with a strong orientation towards applied research.
554 Thanks to the high quality of its reference genome and the existence of large
555 collections of freely available natural accessions collected from the species native
556 range, it also constitutes a prime system for studies in ecology, population genomics
557 and evolutionary biology.

558

559

560 **Experimental procedures**

561 *SNPs calling, population structure and genetic diversity*

562 We used paired-end Illumina sequencing data generated for 44 accessions of
563 *B. distachyon* (Gordon *et al.*, 2017) originating from Spain (N=16), France (N=1),
564 Turkey (N=23) and Iraq (N=4, Table S1 for information about the origin of the
565 accessions and sequencing effort). Reads were aligned to the reference genome v2.0
566 with BWA-MEM (standard settings; Li, 2013). After removing duplicates with
567 Sambamba (Tarasov *et al.*, 2017), single nucleotide polymorphisms (SNPs) were
568 called with Freebayes (Garrison & Marth, 2016). The output was then filtered by
569 removing SNPs with more than 10 missing genotypes or more than 2 alleles, a quality
570 lower than 20, a minor allele frequency of 0.05 and a mean depth lower than 20 or

571 higher than 200. Data were phased using the software BEAGLE V4 (Browning &
572 Browning, 2007) using default settings.

573 We then used the program Admixture (Alexander & Novembre, 2009) to identify the
574 genetic structure of the two populations. The analysis was run for K values from 1 to
575 5, and the best model was determined as the model with the lowest cross-validation
576 error. Summary statistics such as within-population nucleotide or haplotype diversity
577 were computed with the R package PopGenome (Pfeifer *et al.*, 2014). Nucleotide or
578 haplotype diversity values were square-root transformed to fit a normal distribution
579 and a t-test was used to compare the two within-population distributions. Levels of
580 heterozygosity were calculated with VCFtools (Danecek *et al.*, 2011) .

581

582 *Detecting balancing selection with an environmental association analysis*

583 Bioclimatic variables were downloaded at a 30 arc-seconds resolution from
584 <http://www.worldclim.org/> and extracted for each locality using the R libraries gdal
585 and raster. We then picked seven bioclimatic variables (bio6, bio8, bio11, bio12,
586 bio13, bio16, bio18) that displayed substantial variation within geographical groups,
587 but little between them. Bio6, bio8, bio11, bio12, bio13, bio16 and bio18 correspond
588 respectively to minimum temperature of coldest month, mean temperature of wettest
589 quarter, mean temperature of coldest quarter, annual precipitation, precipitation of
590 wettest month, precipitation of wettest quarter and precipitation of warmest quarter.
591 As likely to be correlated, these variables were summarized in a principal components
592 analysis (PCA) in R. The coordinates of the first axis were used to test for correlation
593 between allele frequencies and environment in the R package GENABEL (Aulchenko
594 *et al.*, 2007). We accounted for relatedness between samples using a PCA correction
595 and used corrected P-values of association.

596

597 *Detecting balancing selection with ancestral recombination graphs (ARG)*

598 We used the software ARGWeaver to detect additional candidate regions for
599 balancing selection with a coalescence approach (Rasmussen *et al.*, 2014). We
600 included in the analysis a subset of 12 accessions with high sequencing depth and
601 covering the largest geographical range (6 accessions from each population) to limit
602 computation time. We used a mutation rate of 1.4×10^{-9} /bp/generation, a
603 recombination rate of 5.9×10^{-8} /bp/generation. Mutation rate was estimated by

604 aligning the orthologs of 100 genes and using rice as an out-group (divergence
605 estimated at 40My (The international brachypodium Consortium, 2010)). Note that
606 we subsequently used an outlier approach to identify the oldest polymorphisms
607 present in the two populations (top 1% outliers). Therefore, potential biases inherent
608 to the use of a molecular clock do not affect our analysis. ARGWeaver is also flexible
609 with regard to recombination rate as it reconstructs ancestral recombination graphs
610 and accommodates variable recombination rates and genealogies along the genome.
611 The algorithm was run for 1000 iterations, using 20 discretized time steps, a
612 maximum coalescence time of 3 million generations and a prior effective population
613 size of 100,000 individuals.

614

615 *Detecting disruptive positive selection*

616 We used the Rsb test (Tang *et al.*, 2007) to detect signatures of recent or almost
617 completed hard sweeps. This test detects haplotypes that are positively selected in one
618 population by using a second population as a contrast. While the output of the test
619 provides P-value of significance, it also indicates in which population a given allele is
620 under selection. Rsb statistics were computed for each SNP with the R package
621 rehh2.0 (Gautier *et al.*, 2012) with default settings. We further visualized the
622 extension of haplotypes at candidate regions using the bifurcation.diagram() function
623 of the rehh.

624

625 *Detecting ongoing positive selection within populations*

626 We eventually used the software H-scan (Schlamp *et al.*, 2016) to detect incomplete
627 ongoing positive selection. To do so, we calculated average pairwise haplotypes
628 lengths using the number of segregating sites spanned by each tract within each
629 population. The statistics is expected to be larger as the number of extended
630 haplotypes increases in a population. This method is specifically dedicated to the
631 detection of ongoing sweeps where one (hard sweep) or several (soft sweep)
632 haplotypes are under positive selection and provides statistics for each SNP. We ran
633 the method on Turkish and Spanish accessions independently to detect selective
634 sweeps within each geographical group.

635

636

637 *Testing for functional clustering*

638 We first performed a GO annotation for the 32,712 genes annotated in the reference
639 genome (version 2.1) with Blast2GO (Conesa *et al.*, 2005). We then controlled for
640 potential gene clustering by following the procedure described in (Al-Shahrour *et al.*,
641 2010). The entire gene set of the reference genome was split into windows of 50
642 consecutive genes. Windows were moved along chromosomes in steps of 25 genes to
643 allow for half-window overlaps. Enrichment analyses of biological processes were
644 then performed for all the generated windows with the R package GOstats (Falcon &
645 Gentleman, 2017) using Fisher's exact test. P-values were subsequently adjusted for
646 multiple testing with a Benjamin-Hochberg correction. Regions were considered
647 significantly enriched for a biological process when they displayed a corrected P-
648 value ≤ 0.01 and also harbored at least five genes associated to the given process.

649

650 *GWWS subsequent filtering*

651 Both the H-scan and the Rsb tests compute statistics at each SNP. To limit false
652 positives, we first selected 10 kb windows displaying at least four significant SNPs
653 within the top 1% outliers. Overlapping significant windows were merged. We
654 narrowed down the selected windows by keeping only the genes located at and around
655 (-10% of the peak value) each of the top 1% peaks of selection. For the association
656 test, we also selected 10 kb windows displaying at least four significant SNPs, i.e.
657 with a corrected P-value ≤ 0.001 ($-\log_{10}(\text{P-value}) \geq 3$) and narrowed them down in the
658 same manner. These filtering criteria, however, were not applied to the output of
659 ARGweaver, which is a window-based approach and for which we only kept the top
660 1% outlier windows.

661

662 *Overlap between the different approaches*

663 Venn diagrams were drawn with the R package Vennerable to visualize potential
664 overlap between the different gene sets under selection. To compare the distribution
665 along chromosomes of candidate genes for recent positive selection (H-scan and Rsb
666 candidate genes combined) in each population, we used linear models where the
667 density of selected genes along each chromosome identified in the eastern and
668 western population (100,000 bins per chromosome) were entered as variables. We
669 eventually used the function plotBed of the R package Sushi (Phanstiel, 2015) to

670 visualize the density of genes under positive selection as a heat map along each
671 chromosome. The R package ggplot2 (Wickham, 2009) was used to display the
672 density of all the annotated genes in the genome along each chromosome as a line.

673

674 *Summary statistics and coalescence characterization at candidate loci*

675 Tajima's D , F_{ST} and d_{XY} were computed in the R package PopGenome (v2.2.3) over
676 5kb windows across the genome. We then compared values between windows
677 overlapping with candidate regions and windows outside these regions. We extracted
678 TMRCA and relative TMRCA halftime (RTH) from the output of ARGWeaver.
679 Because the coalescence approach is window-based, summary statistics were
680 averaged across windows including 300 non-recombining blocks (around 10kb
681 windows). Significant windows were merged. We then compared TMRCA and RTH
682 values between windows overlapping with candidate regions and those outside.

683

684 *GO annotation of genes under selection*

685 For each test, we extracted the genes located in the filtered regions with bedtools
686 (Quinlan & Hall, 2010). We then examined potential enrichment for biological
687 processes for each of the selected gene sets with the R package GOstats (Falcon &
688 Gentleman, 2017) using the Fisher's exact test. P-values were subsequently adjusted
689 for multiple testing with a Benjamin-Hochberg correction. Gene sets were considered
690 significantly enriched for a biological process when they displayed a P-value ≤ 0.01
691 and harbored at least five genes associated to the given process. The ancestor and
692 child terms of each significant process were determined using QuickGO
693 (<http://www.ebi.ac.uk/QuickGO>) and used to simplify Fisher test outputs and keep
694 non-redundant terms.

695

696 *QTL for leaf-rust resistance validation*

697 A QTL analysis performed in *B. distachyon* revealed three genomic regions involved
698 in the resistance to *P. brachypodii* (Barbieri *et al.*, 2012). The coordinates of these
699 three QTL were extracted from (Barbieri *et al.*, 2012) from v.2.0 of the *B. distachyon*
700 reference genome. We then assessed whether those three regions were identified as
701 outliers in at least one of the tests of selection.

702

703 **Acknowledgements**

704 We thank the Genetic Diversity Center-ETH Zurich for providing access the Euler
705 high-performance cluster. We also would like to thank Beat Keller's group as well as
706 Simon Krattinger and Mahendra Mariadassou for their advises during the elaboration
707 of the study. This work is supported by the Swiss National Science Foundation
708 (PZ00P3_154724). The work conducted by the U.S. Department of Energy Joint
709 Genome Institute, a DOE Office of Science User Facility, is supported under Contract
710 No. DE-AC02-05CH11231.

711

712 **Availability of data and materials**

713 The raw outputs of each GWWS will be archive upon acceptance of the manuscript.
714 All whole-genome sequences data are available at the NCBI Sequence Read archive
715 (SRA available in Gordon *et al.*, 2017).

716

717 **Conflict of interest**

718 There is no conflict of interest issue related to this work.

719

720 **Supporting Information**

721 Table S1: Geographical coordinates of the 44 accessions and sequencing effort.

722 Table S2: Significant GO terms in each 50 gene-window of the reference genome

723 Table S3: Genes under selection with functional annotation

724

725 **References**

- 726 **Al-Shahrour, Minguéz P, Marques-Bonet T, Gazave E, Navarro A, Dopazo J.**
727 **2010.** Selection upon Genome Architecture: Conservation of Functional
728 Neighborhoods with Changing Genes. *PLoS computational biology* **6**: e1000953.
- 729 **Alexander DH, Novembre J. 2009.** Fast Model-Based Estimation of Ancestry in
730 Unrelated Individuals. *Genome research* **19**: 1655–1664.
- 731 **Aulchenko YS, Ripke S, Isaacs A, van Duijn CM. 2007.** GenABEL: an R library
732 for genome-wide association analysis. *Bioinformatics* **23**: 1294–6.
- 733 **Bakirdere S, Yaman M. 2008.** Determination of lead , cadmium and copper in
734 roadside soil and plants in Elazig , Turkey. *environmental monitoring Assessment*
735 **136**: 401–410.
- 736 **Barbieri M, Marcel TC, Niks RE, Francia E, Pasquariello M, Mazzamurro V,**
737 **Garvin DF. 2012.** QTLs for resistance to the false brome rust *Puccinia brachypodii*
738 in the model grass. *Genome* **163**: 152–163.
- 739 **Bettgenhaeuser J, Gilbert B, Ayliffe M, Moscou MJ. 2014.** Nonhost resistance to
740 rust pathogens – a continuation of continua. *frontiers in plant science* **5**: 1–15.
- 741 **Binney H, Edwards M, Macias-fauria M, Lozhkin A, Anderson P, Kaplan JO,**
742 **Andreev A, Bezrukova E, Blyakharchuk T, Jankovska V, et al. 2017.** Vegetation
743 of Eurasia from the last glacial maximum to present: Key biogeographic patterns.
744 *Quaternary Science Reviews* **157**: 80–97.
- 745 **Bischoff A, Crémieux L, Smilauerova M, Lawson CS, Mortimer SR, Dolezal J,**
746 **Edwards AR, Brook AJ, Macel M, Leps JAN, et al. 2006.** Detecting local
747 adaptation in widespread grassland species – the importance of scale and local plant
748 community. *journal of ecology* **94**: 1130–1142.
- 749 **Bourgeois Y, Roulin AC, Müller K, Ebert D. 2017.** Parasitism drives host genome
750 evolution: Insights from the *Pasteuria ramosa* - *Daphnia magna* system. *Evolution*
751 **71**:1106–13.
- 752 **Brown JKM, Tellier A. 2011.** Plant-parasite coevolution: bridging the gap between
753 genetics and ecology. *Annual Review of Phytopathology* **49**: 345–67.
- 754 **Browning SR, Browning BL. 2007.** Rapid and Accurate Haplotype Phasing and
755 Missing-Data Inference for Whole-Genome Association Studies By Use of
756 Localized Haplotype Clustering. *the american journal of human genetics* **81**: 1084–
757 1097.
- 758 **Carmo S Do, Charron J. 2014.** Comparative analysis of the cold acclimation and

- 759 freezing tolerance capacities of seven diploid *Brachypodium distachyon* accessions.
760 *Annals of botany* **113**: 681–693.
- 761 **Ceballos, G., Davidson, A., List, R., Pacheco, J., Manzano-Fisher, P., Santos-**
762 **Barrera, G., Cruzado J. 2010.** Rapid Decline of a Grassland System and Its
763 Ecological and Conservation Implications. *PloS one* **5**: e8562.
- 764 **Charlesworth D. 2006.** Balancing selection and its effects on sequences in nearby
765 genome regions. *PLoS Genetics* **2**: e64.
- 766 **Chavan S, Gray J, Smith SM. 2015.** Diversity and evolution of Rp1 rust resistance
767 genes in four maize lines. *Theoretical and Applied Genetics* **128**: 985–998.
- 768 **Clayton WD. 1981.** Evolution and Distribution of Grasses. *Annals of the Missouri*
769 *Botanical Garden* **68**: 5–14.
- 770 **Conesa A, Götz S, García-Gómez JM, Terol J, Talón M, Robles M. 2005.**
771 Blast2GO: a universal tool for annotation, visualization and analysis in functional
772 genomics research. *Bioinformatics* **21**: 3674–6.
- 773 **Couto D, Zipfel C. 2016.** Regulation of pattern recognition receptor signalling in
774 plants. *nature reviews immunology* **16**: 537–552.
- 775 **Cruickshank TE, Hahn MW. 2014.** Reanalysis suggests that genomic islands of
776 speciation are due to reduced diversity, not reduced gene flow. *Molecular Ecology*
777 **23**: 3133–3157.
- 778 **Cutter AD, Payseur BA. 2013.** Genomic signatures of selection at linked sites□:
779 unifying the disparity among species. *Nature reviews Genetics* **14**: 262–274.
- 780 **Danecek P, Auton A, Abecasis G, Albers CA, Banks E, Depristo MA, Handsaker**
781 **RE, Lunter G, Marth GT, Sherry ST, et al. 2011.** The variant call format and
782 VCFtools. *Bioinformatics* **27**: 2156–2158.
- 783 **Dell'Acqua MD, Zuccolo A, Tuna M, Gianfranceschi L, Pè ME. 2014.** Targeting
784 environmental adaptation in the monocot model *Brachypodium distachyon*□: a
785 multi-faceted approach. *BMC Genomics* **15**: 801.
- 786 **Delph LF, Kelly JK. 2014.** On the importance of balancing selection in plants Lynda.
787 *New phytologist* **201**: 1–22.
- 788 **Des Marais DL, Juenger TE. 2015.** *Brachypodium* and the Abiotic Environment. In:
789 Vogel J, editor. *Genetics and Genomics of Brachypodium*, 291–311.
- 790 **Dodds P, Thrall P. 2009.** Recognition events and host–pathogen co-evolution in
791 gene-for- gene resistance to flax rust. *Functional plant biology* **36**: 395–408.
- 792 **Dong S, Raffaele S, Kamoun S. 2015.** ScienceDirect The two-speed genomes of

- 793 filamentous pathogens: waltz with plants. *Current Opinion in Genetics &*
794 *Development* **35**: 57–65.
- 795 **Durian G, Rahikainen M, Alegre S, Brosché M. 2016.** Protein Phosphatase 2A in
796 the Regulatory Network Underlying Biotic Stress Resistance in Plants. *frontiers in*
797 *immunology* **7**: 1–17.
- 798 **Eckardt NA. 2017.** The Plant Cell Reviews Plant Immunity: Receptor-Like
799 Kinases, ROS-RLK Crosstalk, Quantitative Resistance, and the Growth / Defense
800 Trade-Off. *Plant cell* **29**: 601–602.
- 801 **Falcon SÃ, Gentleman R. 2017.** Using GOSTats to test gene lists for GO term
802 association. *Bioinformatics* **23**: 257–258.
- 803 **Feder ME, Mitchell-olds T. 2003.** Evolutionary and ecological functional genomics.
804 *Nature reviews Genetics* **4**: 649–655.
- 805 **Feliner GN. 2011.** Southern European glacial refugia: A tale of tales. *taxon* **60**:
806 365–372.
- 807 **Fijarczyk A, Babik A. 2015.** Detecting balancing selection in genomes: limits and
808 prospects. *Molecular ecology* **24**: 3529–3545.
- 809 **Flood J, Hancock AM. 2017.** ScienceDirect The genomic basis of adaptation in
810 plants. *Current opinion in plant biology* **36**: 88–94.
- 811 **Fones H, Preston GM. 2011.** Reactive oxygen and oxidative stress tolerance in plant
812 pathogenic Pseudomonas. *FEMS Microbiology letter* **1**: 1–8.
- 813 **Fuller ZL, Niño EL, Patch HM, Bedoya-Reina OC, Baumgarten T, Muli E,**
814 **Mumoki F, Ratan A, McGraw J, Frazier M, et al. 2015.** Genome-wide analysis
815 of signatures of selection in populations of African honey bees (*Apis mellifera*)
816 using new web-based tools. *BMC genomics* **16**: 518.
- 817 **Fumagalli M, Sironi M, Pozzoli U, Ferrer-admettla A, Pattini L. 2011.** Signatures
818 of Environmental Genetic Adaptation Pinpoint Pathogens as the Main Selective
819 Pressure through Human Evolution. *PLoS genetics* **7**: e1002355.
- 820 **Garrison E, Marth G. 2016.** Haplotype-based variant detection from short-read
821 sequencing. Available at:<https://arxiv.org/abs/1207.3907>
- 822 **Gautier M, Vitalis R, Baillarguet D, Cedex F-M. 2012.** rehh: an R package to
823 detect footprints of selection in genome-wide SNP data from haplotype structure.
824 *Bioinformatics* **28**: 1176–1177.
- 825 **Gibson DJ. 2009.** *Grasses and grassland ecology* (Oxford university press, Ed.).
- 826 **Gordon SP, Contreras-Moreira B, Woods DP, Des Marais DL, Burgess D, Shu S,**

- 827 **Stritt C, Roulin AC, Schackwitz W, Tyler et al.** Extensive gene content
828 hetlvariation in the *Brachypodium distachyon* pan-genome correlates with
829 phenotypic variation. *Nature Communications* **8**: 2184
- 830 **Gordon SP, Priest H, Marais DL Des, Schackwitz W, Figueroa M, Martin J,**
831 **Jennifer N, Tyler L, Lee C, Bryant D, et al. 2014.** Genome diversity in
832 *Brachypodium distachyon*: deep sequencing of highly diverse inbred lines. *Plant*
833 *Journal* **79**: 361–374.
- 834 **Gos G, Slotte T, Wright SI. 2012.** Signatures of balancing selection are maintained
835 at disease resistance loci following mating system evolution and a population
836 bottleneck in the genus *Capsella*. *BMC Evolutionary Biology* **12**: 152.
- 837 **Greeff C, Roux M, Mundy J, Petersen M. 2012.** Receptor-like kinase complexes in
838 plant innate immunity. *frontiers in plant science* **3**: 1–7.
- 839 **Groves RH. 2000.** Temperate grasslands of the southern hemisphere. In: Jacobs
840 SWL, Everett J, editors. *Grasses Systematics and Evolution*, 3781–3791.
- 841 **Hammond-kosack KE, Jones JDG. 1996.** Resistance Gene-Dependent Plant
842 Defense Responses. *The Plant cell* **8**: 1773–1791.
- 843 **Hancock AM, Brachi B, Faure N, Horton MW, Jarymowycz LB, Sperone FG,**
844 **Toomajian C, Roux F, Bergelson J. 2011.** Adaptation to climate across the
845 *Arabidopsis thaliana* genome. *Science* **334**: 83–6.
- 846 **Hassl RJ, Payseur BA. 2016.** Detecting selection in natural populations: Making
847 sense of genome scans and towards alternative solutions. *Molecular Ecology* **25**: 5–
848 23.
- 849 **Helm A, Oja T, Saar L, Takkis K, Talve T, Pa M. 2009.** Human influence lowers
850 plant genetic diversity in communities with extinction debt. *journal of ecology* **97**:
851 1329–1336.
- 852 **Hermisson J. 2009.** Who believes in whole-genome scans for selection? *Heredity*
853 **103**: 283–284.
- 854 **Hewitt GM. 1999.** Post-glacial re-colonization of European biota. *Biological journal*
855 *of the Linnean society* **68**: 87–112.
- 856 **Hewitt G. 2000.** The genetic legacy of the Quaternary ice ages. *Nature* **405**: 907–913.
- 857 **Hovmøller MS, Sørensen CK, Walter S, Justesen AF. 2011.** Diversity of *Puccinia*
858 *striiformis* on Cereals and Grasses. *Annual Review of Phytopathology* **49**: 197–220.
- 859 **Huang J, Pray C, Rozelle S. 2002.** Enhancing the crops to feed the poor. *Nature*
860 **418**: 678–684.

- 861 **Huo N, Garvin DF, You FM, Luo SMM, Gu YQ, Lazo GR, Philip J. 2011.**
862 Comparison of a high-density genetic linkage map to genome features in the model
863 grass *Brachypodium distachyon*. *Theoretical and Applied Genetics* **123**: 455–464.
- 864 **Jacob F, Vernaldi S, Maekawa T. 2013.** Evolution and conservation of plant NLR
865 functions. *frontiers in immunology* **4**: 1–16.
- 866 **Karasov TL, Horton MW, Bergelson J.** ScienceDirect Genomic variability as a
867 driver of plant – pathogen coevolution? *Current Opinion in Plant Biology* **18**: 24–
868 30.
- 869 **Kelley JL, Madeoy J, Calhoun JC, Swanson W, Akey JM. 2006.** Genomic
870 signatures of positive selection in humans and the limits of outlier approaches.
871 *Genome research*: **206**: 980–989.
- 872 **Kiviniemi K, Eriksson O. 2002.** Size-related deterioration of semi-natural grassland
873 fragments in Sweden. *diversity and distribution* **8**: 21–29.
- 874 **Krattinger SG, Keller B. 2016a.** Tansley review Molecular genetics and evolution
875 of disease resistance in cereals. *New phytologist*: 320–332.
- 876 **Krattinger SG, Keller B. 2016b.** Trapping the intruder — immune receptor domain
877 fusions provide new molecular leads for improving disease resistance in plants.
878 *Genome Biology* **17**:23.
- 879 **Latta RG. 2009.** Testing for local adaptation in *Avena barbata*: a classic example of
880 ecotypic divergence. *Molecular Ecology* **18**: 3781–3791.
- 881 **Li H. 2013.** Aligning sequence reads, clone sequences and assembly contigs with
882 BWA-MEM. preprint arXiv:1303.3997.
- 883 **Liu W, Frick M, Huel R, Nykiforuk CL, Wang X, Gaudet DA, Eudes F, Conner
884 RL, Kuzyk A, Chen Q, et al. 2014.** The Stripe Rust Resistance Gene Yr10 Encodes
885 an Evolutionary-Conserved and Unique CC – NBS – LRR Sequence in Wheat.
886 *Molecular Plant* **7**: 1740–1755.
- 887 **Long Q, Rabanal FA, Meng D, Huber CD, Farlow A, Platzer A, Zhang Q,
888 Vilhjálmsson BJ, Korte A, Nizhynska V, et al. 2013.** Massive genomic variation
889 and strong selection in *Arabidopsis thaliana* lines from Sweden. *Nature genetics* **45**:
890 884–890.
- 891 **Lopez-Alvarez D, Manzaneda AJ, Rey P, Giraldo P, Benavente E,
892 Allainguillaume J et al. 2015.** Environmental niche variation and evolutionary
893 diversification of the *Brachypodium distachyon* grass complex species in their
894 native. *American journal of botany* **102**: 1073–1088.

- 895 **Luo N, Liu J, Yu X, Jiang Y. 2011.** Natural variation of drought response in
896 *Brachypodium distachyon*. *physiologia plantarum* **141**: 19–29.
- 897 **Mace E, Tai S, Innes D, Godwin I, Hu W, Campbell B, Gilding E, Cruickshank**
898 **A, Prentis P, Wang J, et al. 2014.** The plasticity of NBS resistance genes in
899 sorghum is driven by multiple evolutionary processes. *BMC plant biology* **14**: 253.
- 900 **Manzaneda AJ, Rey PJ, Bastida JM, Weiss-Lehman C, Raskin E, Mitchell-Olds**
901 **T. 2013.** Environmental aridity is associated with cytotype segregation and
902 polyploidy occurrence in *Brachypodium distachyon* (Poaceae) Antonio. *New*
903 *phytologist* **193**: 797–805.
- 904 **Mchale L, Tan X, Koehl P, Michelmore RW. 2006.** Plant NBS-LRR proteins □:
905 adaptable guards. *Genome Biology* **7**: 212.
- 906 **Messer PW. 2015.** H-scan □: Detecting hard and soft sweeps in population genomic
907 data. **3**: 1–4.
- 908 **Michelmore RW, Meyers BC. 1998.** Clusters of Resistance Genes in Plants Evolve
909 by Divergent Selection and a Birth-and-Death Process. *Genome research* **530**:
910 1113–1130.
- 911 **Mitchell-Olds T, Willis JH, Goldstein DB. 2007.** Which evolutionary processes
912 influence natural genetic variation for phenotypic traits? *Nature reviews Genetics* **8**:
913 845–56.
- 914 **Mondragón-palomino M, Meyers BC, Michelmore RW, Gaut BS. 2002.** Patterns
915 of Positive Selection in the Complete NBS-LRR Gene Family of *Arabidopsis*
916 *thaliana*. *Genome research* **12**: 1305–1315.
- 917 **Mor F, Ceylan S. 2017.** Cadmium and lead contamination in vegetables collected
918 from industrial , traffic and rural areas in Bursa Province, Turkey. *Food Additives &*
919 *Contaminants* □ **25**: 611–615.
- 920 **Morris GP, Ramu P, Deshpande SP, Hash CT, Shah T, Upadhyaya HD. 2013.**
921 Population genomic and genome-wide association studies of agroclimatic traits in
922 sorghum. *Proceedings of the National Academy of Sciences* **110**: 453–458.
- 923 **Mur LAJ, Bosch M. 2016.** Linking Dynamic Phenotyping with Metabolite Analysis
924 to Study Natural Variation in Drought Responses of *Brachypodium distachyon*.
925 *frontiers in plant science* **7**: 1–15.
- 926 **Nelson RM, Wallberg A, Sim P, Lawson DJ, Webster MT. 2017.** Genomewide
927 analysis of admixture and adaptation in the Africanized honeybee. *Molecular*
928 *Ecology* **26**: 3603–3617.

- 929 **Nielsen R. 2005.** Molecular Signatures of Natural Selection. *Annual Review of*
930 *Genetics.* **39**: 197–218.
- 931 **Nutzmann H, Osbourn A. 2014.** Gene clustering in plant specialized metabolism.
932 *current opinion in biotechnology* **26**: 91–99.
- 933 **Ooijen G Van, Mayr G, Kasiem MMA, Albrecht M, Cornelissen BJC, Takken**
934 **FLW. 2017.** Structure – function analysis of the NB-ARC domain of plant disease
935 resistance proteins. *journal of experimental botany* **59**: 1383–1397.
- 936 **Opanowicz M, Vain P, Draper J, Parker D, Doonan JH. 2008.** Brachypodium
937 distachyon: making hay with a wild grass. *Trends in Plant Science* **13**: 172–177.
- 938 **País SM, Téllez-iñón MT, Capiati DA. 2009.** Serine / threonine protein
939 phosphatases type 2A and their roles in stress signaling. *Plant signaling and*
940 *behaviour* **4**: 1013–1015.
- 941 **Park C, Caddell DF, Ronald PC. 2012.** Protein phosphorylation in plant
942 immunity: insights into the regulation of pattern recognition receptor-mediated
943 signaling. *frontiers in plant science* **3**: 1–9.
- 944 **Pavlidis P, Jensen JD, Stephan W, Stamatakis A. 2012.** A Critical Assessment of
945 Storytelling: Gene Ontology Categories and the Importance of Validating
946 Genomic Scans Research article. *Molecular biology and evolution* **29**: 3237–3248.
- 947 **Phanstiel DH. 2015.** Sushi: Tools for visualizing genomics data. *R package version*
948 *1.14.0*.
- 949 **Pfeifer B, Wittelsbürger U, Ramos-Onsins SE, Lercher MJ. 2014.** PopGenome:
950 An efficient swiss army knife for population genomic analyses in R. *Molecular*
951 *Biology and Evolution* **31**: 1929–1936.
- 952 **Platt A, Horton M, Huang YS, Li Y, Anastasio AE, Mulyati NW, Bossdorf O,**
953 **Byers D, Donohue K, Dunning M, et al. 2010.** The Scale of Population Structure
954 in *Arabidopsis thaliana*. *plos genetics* **6**: e1000843.
- 955 **Quinlan AR, Hall IM. 2010.** BEDTools: a flexible suite of utilities for comparing
956 genomic features. *Bioinformatics* **26**: 841–842.
- 957 **Rasmussen MD, Hubisz MJ, Gronau I, Siepel A. 2014.** Genome-Wide Inference of
958 Ancestral Recombination Graphs. *PLoS genetics* **10**: e1004342.
- 959 **Renaut S, Grassa CJ, Yeaman S, Moyers BT, Lai Z, Kane NC, Bowers JE, Burke**
960 **JM, Rieseberg LH. 2013.** Genomic islands of divergence are not affected by
961 geography of speciation in sunflowers. *Nature Communications* **4**: 1–8.
- 962 **Richman A. 2000.** Evolution of balanced genetic polymorphism. *Molecular Ecology*

- 963 **9:** 1953–1963.
- 964 **Roulin A, Bourgeois Y, Stiefel U, Walser J-C, Ebert D.** A photoreceptor underlies
965 natural variation in *Daphnia magna* diapause induction. *Molecular Biology and*
966 *Evolution.* **12:**3194–3204.
- 967 **Samuk K, Rennison DJ, Owens GL, Delmore KE, Miller SE, Schluter D. 2017.**
968 Gene flow and selection interact to promote adaptive divergence in regions of low
969 recombination. *Molecular Ecology* **26:** 4378–4390.
- 970 **Savolainen O, Lascoux M, Merilä J. 2013.** Ecological genomics of local adaptation.
971 *Nature reviews Genetics* **14:** 807–820.
- 972 **Schlamp F, Van Der Made J, Stambler R. 2016.** Evaluating the performance of
973 selection scans to detect selective sweeps in domestic dogs. *Molecular Ecology* **25:**
974 342–356.
- 975 **Sewelam N, Kazan K, Schenk PM. 2016.** Global Plant Stress Signaling□: Reactive
976 Oxygen Species at the. **7:** 1–21.
- 977 **Singh S, Chand S, Singh NK, Sharma TR. 2015.** Genome-Wide Distribution ,
978 Organisation and Functional Characterization of Disease Resistance and Defence
979 Response Genes across Rice Species. *Plos one* **10:**e0125964
- 980 **Slavov GT, Nipper R, Robson P, Farrar K, Allison GG, Bosch M, Clifton-brown**
981 **JC, Donnison IS, Jensen E. 2014.** Genome-wide association studies and prediction
982 of 17 traits related to phenology, biomass and cell wall composition in the energy
983 grass *Miscanthus sinensis*. *New phytologist* **201:** 1227–1239.
- 984 **Slotte T. 2014.** The impact of linked selection on plant genomic variation. *briefings*
985 *in functional genomics* **13:** 268–275.
- 986 **Stamatakis A, Alachiotis N, Pavlidis P, Daniel Z. 2013.** SweeD□: Likelihood-
987 Based Detection of Selective Sweeps in Thousands of Genomes. *Molecular biology*
988 *and evolution* **30:** 2224–2234.
- 989 **Stinchcombe JR, Hoekstra HE. 2008.** Combining population genomics and
990 quantitative genetics: finding the genes underlying ecologically important traits.
991 *Heredity* **100:** 158–170.
- 992 **Stritt C, Gordon SP, Wicker T, Vogel JP, Roulin AC.** Transposable elements as a
993 major source of genetic diversity: insights from genome-wide analyses of
994 *Brachypodium distachyon* natural accessions. *Genome biology and evolution.* In
995 press. Available at <https://doi.org/10.1093/gbe/evx276>.
- 996 **Stromberg C. 2011.** Evolution of Grasses and Grassland Ecosystems. *Annual review*

- 997 *of earth and planetary science* **39**: 517–544.
- 998 **Stukenbrock EH, Banke S, Javan-nikkhah M, Mcdonald BA. 2005.** Origin and
999 Domestication of the Fungal Wheat Pathogen *Mycosphaerella graminicola* via
1000 Sympatric Speciation. *Molecular biology and evolution* **24**: 398–411.
- 1001 **Sun J, Hu W, Zhou R, Wang L. 2015.** The Brachypodium distachyon BdWRKY36
1002 gene confers tolerance to drought stress in transgenic tobacco plants. *Plant cell*
1003 *reports* **34**: 23–35.
- 1004 **Svenning J, Normand S, Kageyama M. 2008.** Glacial refugia of temperate trees in
1005 Europe: insights from species distribution modelling. *journal of ecology* **96**: 1117–
1006 1127.
- 1007 **Tajima F. 1989.** Statistical method for testing the neutral mutation hypothesis by
1008 DNA polymorphism. *Genetics* **123**: 585–95.
- 1009 **Takos AM, Knudsen C, Lai D, Kannangara R, Mikkelsen L, Motawia MS, Olsen**
1010 **CE, Sato S, Tabata S, Jørgensen K, et al. 2011.** Genomic clustering of cyanogenic
1011 glucoside biosynthetic genes aids their identification in *Lotus japonicus* and
1012 suggests the repeated evolution of this chemical defence pathway. *Plant Journal* **68**:
1013 273–286.
- 1014 **Tang K, Thornton KR, Stoneking M. 2007.** A New Approach for Using Genome
1015 Scans to Detect Recent Positive Selection in the Human Genome. *PLoS biology*
1016 **5**:e171
- 1017 **Tarasov A, Vilella AJ, Cuppen E, Nijman IJ, Prins P. 2017.** Genome analysis
1018 Sambamba: fast processing of NGS alignment formats. *Bioinformatics* **31**: 2032–
1019 2034.
- 1020 **The international brachypodium Consortium. 2010.** Genome sequencing and
1021 analysis of the model grass *Brachypodium distachyon*. *Nature* **463**: 763–8.
- 1022 **Torres MA, Jones JDG, Dangl JL. 2006.** Reactive Oxygen Species Signaling in
1023 Response to Pathogens. **141**: 373–378.
- 1024 **Turchin MC, Chiang CWK, Palmer CD, Sankararaman S, Reich D,**
1025 **Investigation G, Giant T, Hirschhorn JN. 2012.** Evidence of widespread selection
1026 on standing variation in Europe at height-associated SNPs. *Nature Genetics* **44**:
1027 1015–1019.
- 1028 **Tyler AL, Lee SJ, Young ND, Deiulio GA, Benavente E, Reagon M, Sysopha J,**
1029 **Baldini RM, Troia A, Hazen SP, et al. 2016.** Population structure in the model
1030 grass *Brachypodium distachyon* is highly correlated with flowering differences

1031 across broad geographic areas. *The Plant Genome* **9**:1–55.

1032 **Wadgymar SM, Lowry DB, Gould BA, Byron CN, Mactavish RM, Anderson JT.**

1033 **2017.** Identifying targets and agents of selection: innovative methods to evaluate the

1034 processes that contribute to local adaptation. *Methods in Ecology and Evolution* **8**:

1035 738–749.

1036 **Wallace JS, Batchelor CH. 1997.** Managing water resources for crop production.

1037 *Philosophical transactions of the Royal Society of London. Series B, Biological*

1038 *sciences* **352**: 937–947.

1039 **Wickham H. 2009.** ggplot2: Elegant Graphics for Data Analysis. Springer-Verlag

1040 New York.

1041 **Wojtaszek P. 1997.** Oxidative burst□: an early plant response to pathogen infection.

1042 *biochemical journal* **692**: 681–692.

1043 **Wu Q, Han T, Chen X, Chen J, Zou Y, Li Z, Xu Y. 2017.** Long-term balancing

1044 selection contributes to adaptation in Arabidopsis and its relatives. *Genome biology*

1045 **18**: 217.

1046 **Wyand RA, Brown K. 2003.** Genetic and forma specialis diversity in Blumeria

1047 graminis of cereals and its implications for host-pathogen co-evolution. *Molecular*

1048 *plant pathology* **4**: 187–198.

1049 **Zhong Y, Li Y, Huang K, Cheng Z. 2015.** Species-specific duplications of NBS-

1050 encoding genes in Chinese chestnut (*Castanea mollissima*). *Scientific reports* **5**:

1051 16638.

1052

1053

1054

1055

1056

1057

1058

1059

1060

1061

1062

1063

1064

1065 **Figures**

1066

1067 **Figure 1: Schematic representation of the regimes of selection analyzed in this**
1068 **study**

1069 In the case of association between SNPs and environmental variables displaying
1070 variation within population, shared polymorphisms will be maintained across the two
1071 populations. The same outcome is expected under long-term balancing selection. The
1072 Rsb test, on the other hand, detects mutations that rose in frequency and reached near
1073 fixation in one of the two populations. The H-scan test targets mutations currently
1074 under selection and rising in frequency in one of the two populations.

1075

1076 **Figure 2: Geographical origin and genetic diversity of the 44 accessions**

1077 A) Geographical origin of the 44 accessions used in the study. Blue and orange dots
1078 represent accessions from the western and eastern population respectively. The
1079 asterisk indicates the origin of the reference accession Bd21 B) Structure plot. Each
1080 bar represents the genetic data of one accession. An accession presents some
1081 admixture when the bar displays different colors. The high of the bar is proportional
1082 to the admixture level C) Nucleotide diversity (in 5 kb windows) with the eastern and
1083 western population D) PCA summarizing bioclimatic variables varying within the
1084 eastern and western population.

1085

1086 **Figure 3: Venn diagram and descriptive statistics for each test of selection**

1087 A) Overlap between environmental association, H-scan and Rsb results in the eastern
1088 and western populations, in number of genes B) Number of genes per window after
1089 keeping the genes located at and in the vicinity of each peak of selection C)
1090 Comparison between genome-wide (GW) Tajima's D and Tajima's D in regions
1091 under the different selection regimes tested D) Overall gene density (line) and heat
1092 maps displaying the density of genes under positive selection (Rsb + H-scan) along
1093 the five chromosomes in the eastern (E) and western (W) populations.

1094

1095 **Figure 4: QTL involved in resistance to rust**

1096 A) Rsb signals observed in QTL_{rust-3} (left panel) and QTL_{rust-4} (right panel). The
1097 dashed line indicates the 0.1% $-\log_{10}(\text{Rsb P-values})$ outlier threshold. Note that in
1098 order to reduce the size of the figure, points with $-\log_{10}(\text{Rsb P-values})$ values <1 are
1099 not displayed. Grey boxes display the position of gene potentially involved in defense

1100 response (genes with NBS-LRR, F-box or RLK domains) if present in the region B)
1101 Haplotype bifurcation diagram in sub-regions displaying strong Rsb outliers. Left
1102 panel: zoom in on chromosome 3; right panel: zoom in on chromosome 4. The
1103 diagrams visualize the breakdown of LD at increasing distances from the selected
1104 focal SNP, displayed by a vertical black line. Each horizontal blue line represents a
1105 haplotype. Each accession is represented by two lines, one for each haplotype.
1106 Horizontal blue lines are merged when two accessions share the same haplotype. The
1107 thickness of the line is therefore correlated to the number of accessions sharing the
1108 same haplotype.

1109

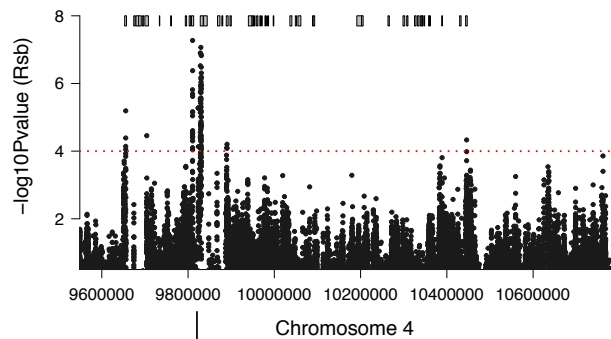
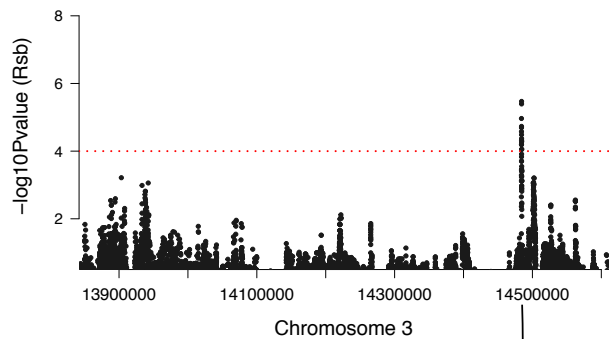
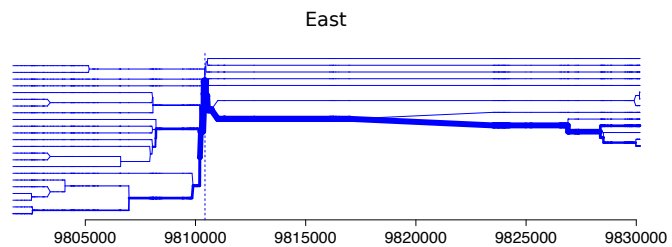
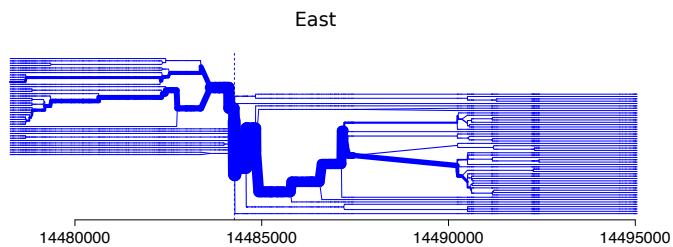
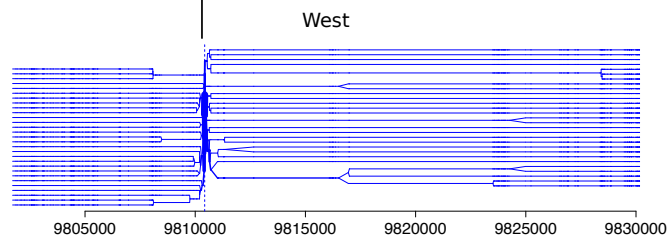
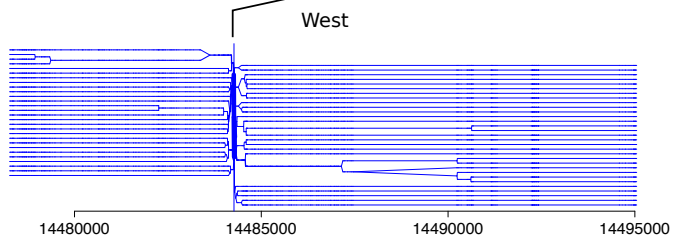
1110

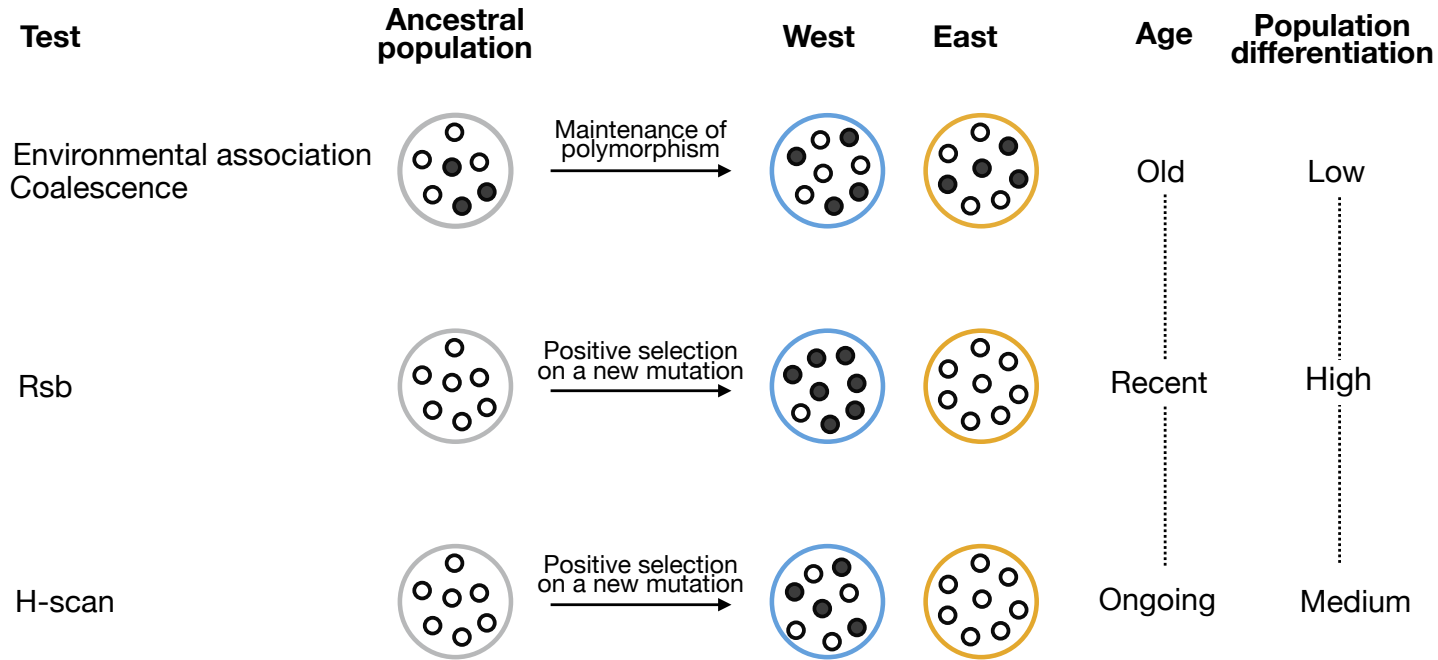
1111 **Tables**

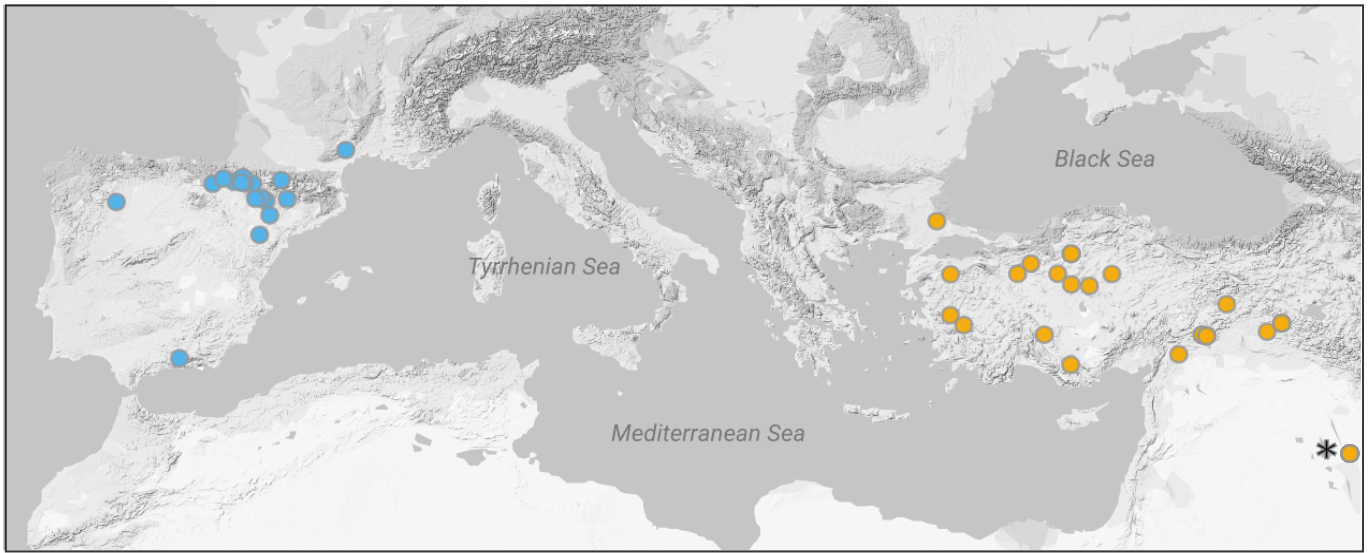
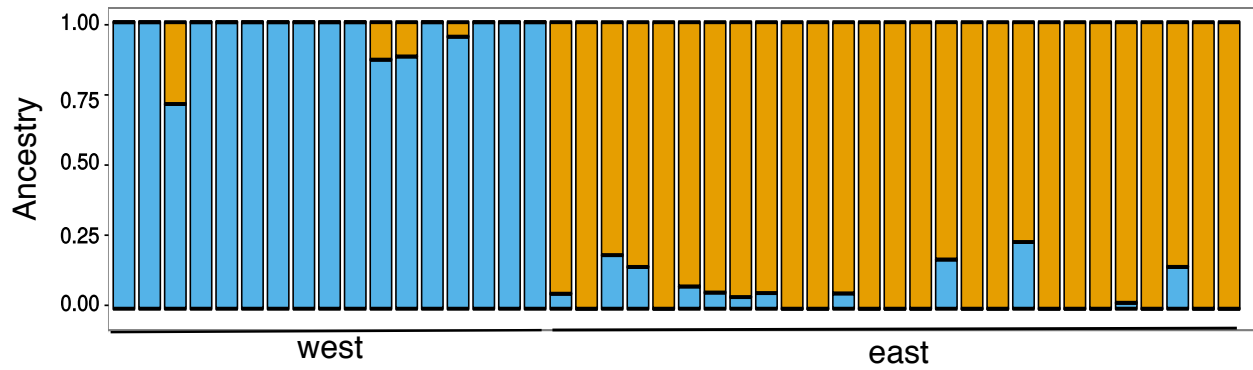
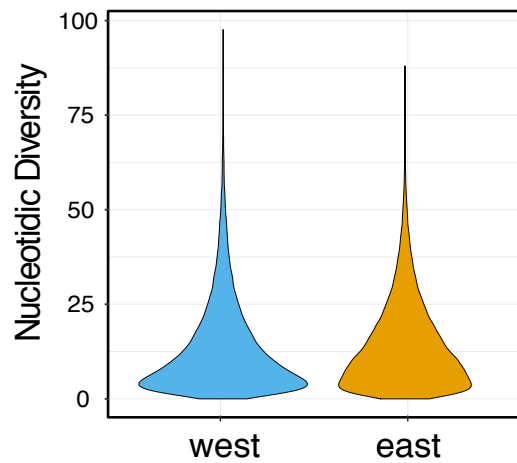
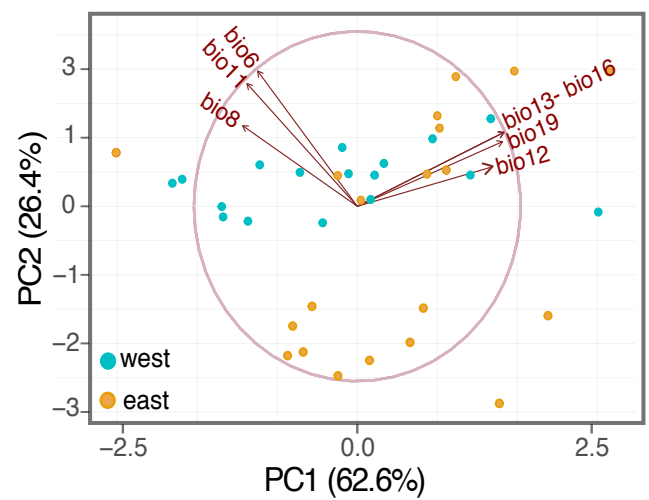
1112 **Table 1: Significant GO term associated to each test of selection**

1113

1114

A**B**



A**B****C****D**

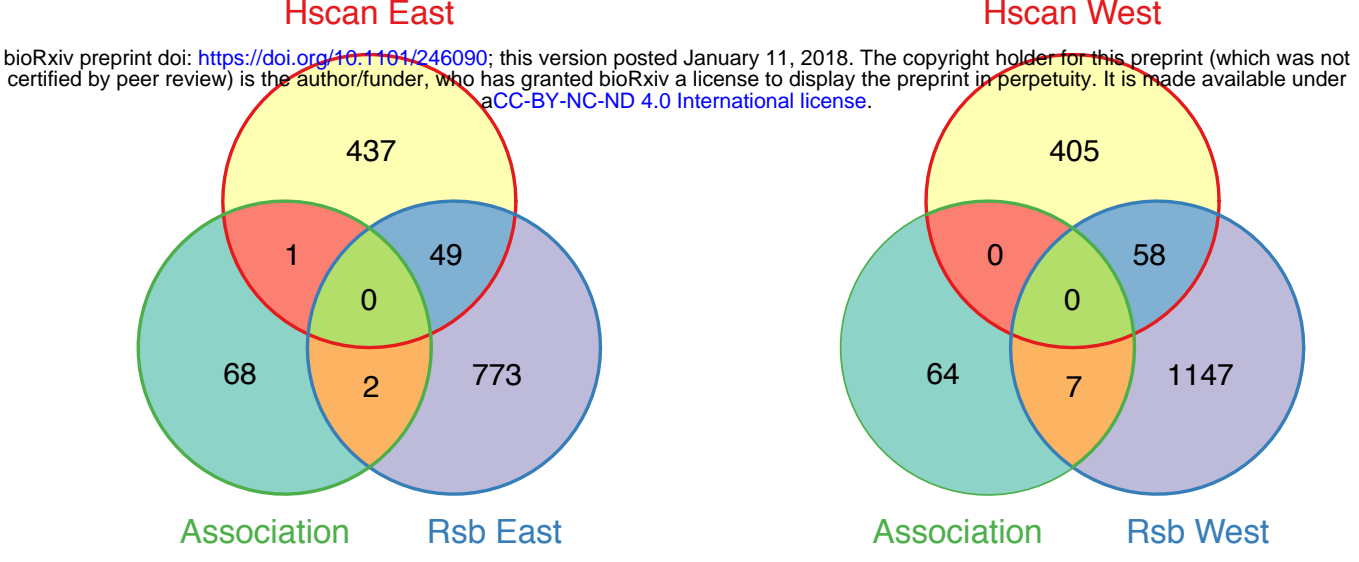
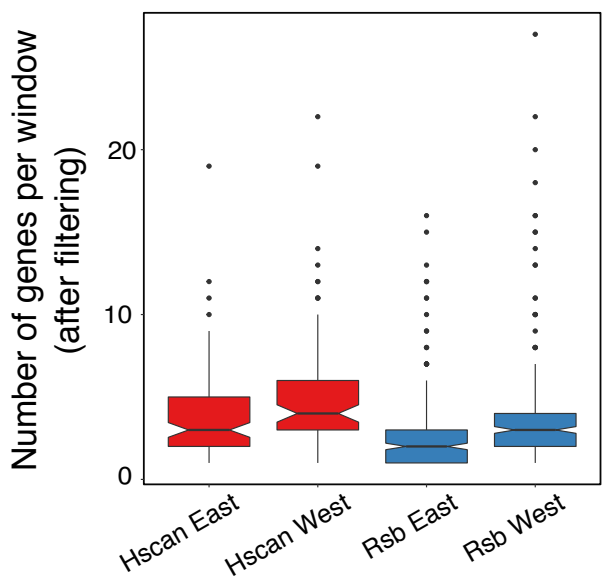
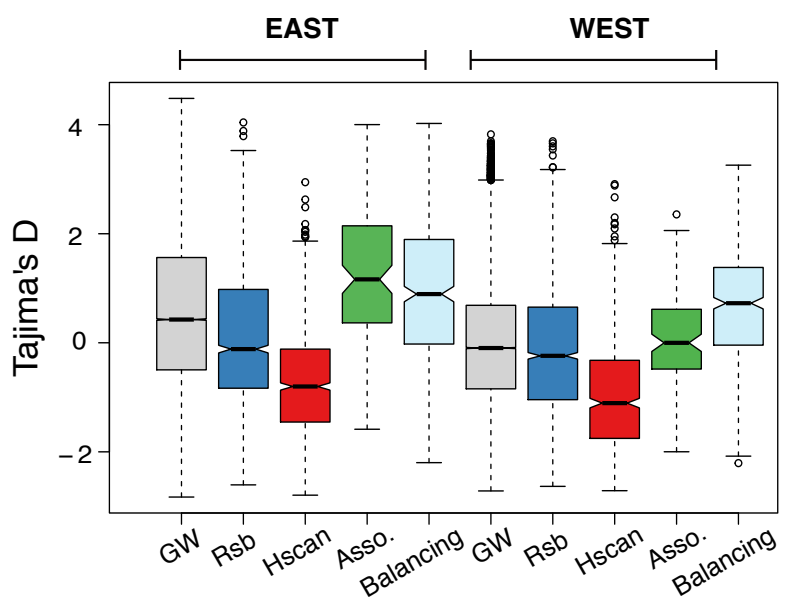
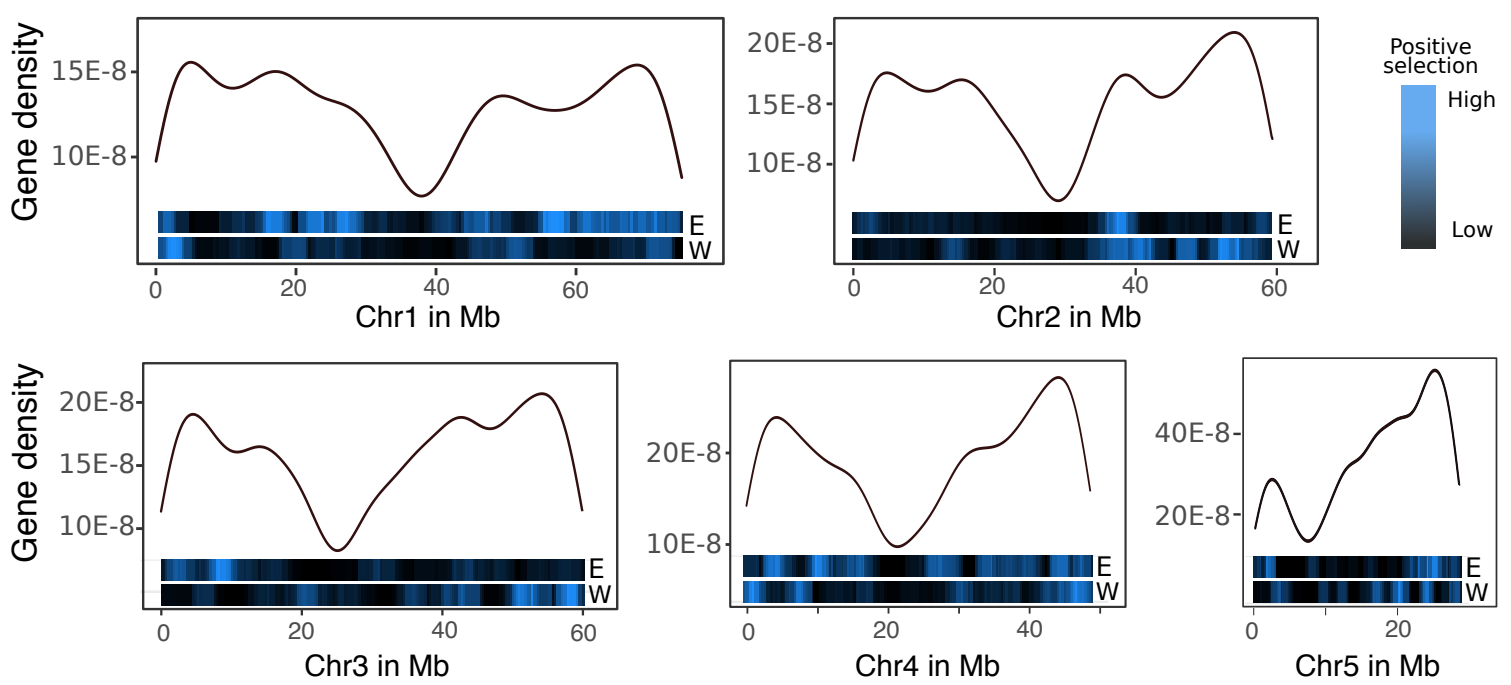
A**B****C****D**

Table 1: significant GO term associated to each test of selection

Test	Significant GO process	Pvalue
Association	None	NA
TMRCA	Phosphorylation	3.13E-08
Rsb East	Response to stress including: - defense response - response to oxidative stress	3.00E-05 2.98E-03 2.98E-03
RsbWest	Nitrogen compound transport	4.70E-03
H-scan East	Response to stress including: - defense response - response to cadmium ion	2.66E-04 7.82E-05 2.66E-04
H-scan West	Pyruvate metabolic process	4.00E-04